

# Patterning surfaces with functional polymers

The ability to pattern functional polymers at different length scales is important for research fields including cell biology, tissue engineering and medicinal science and the development of optics and electronics. The interest and capabilities of polymer patterning have originated from the abundance of functionalities of polymers and a wide range of applications of the patterns. This paper reviews recent advances in top-down and bottom-up patterning of polymers using photolithography, printing techniques, self-assembly of block copolymers and instability-induced patterning. Finally, challenges and future directions are discussed from the point of view of both applicability and strategies for the surface patterning of polymers.

## ZHIHONG NIE<sup>1</sup> AND EUGENIA KUMACHEVA<sup>1,2,3</sup>

<sup>1</sup>Department of Chemistry, University of Toronto, 80 Saint George Street, Toronto, Ontario M5S 3H6, Canada

<sup>2</sup>Department of Chemical Engineering and Applied Chemistry, University of Toronto, 200 College Street, Toronto, Ontario M5S 3E5, Canada

<sup>3</sup>Institute of Biomaterials & Biomedical Engineering University of Toronto, Taddle Creek Road, Toronto, Ontario M5S 3G9, Canada

e-mail: ekumache@chem.utoronto.ca

The past decade has witnessed the rapid development of a broad range of strategies used to pattern polymers. Intense interest in polymer patterning originated from the diversity of existing synthetic and biological polymers, and the ability to ‘design’ new types of polymers so that various functions of polymer-patterned surfaces can be readily addressed. Polymer patterns typically have high fidelity, owing to the suppressed lateral diffusion of macromolecules. High-resolution polymer patterns can be produced by patterning reactive precursor molecules and polymerizing them directly on the surface. A truly unique approach to surface patterning has been realized through the self-assembly of block copolymers. Polymers have relatively low cost, good mechanical properties and are compatible with most patterning techniques.

The applications of polymer-patterned surfaces can be tentatively organized into several categories: (1) the fabrication of light-emitting displays (LEDs), semiconductor microelectronics and plastic electronics<sup>1–3</sup>; (2) bio-related and medicinal research including the study of cells and tissue engineering<sup>4–6</sup>; (3) the generation of masks and templates<sup>7,8</sup>; (4) the production of optical components such as gratings or photonic crystals<sup>9,10</sup>; and (5) fundamental research in surface science and combinatorial synthesis<sup>11,12</sup>.

In this review, we highlight recent advances in top-down and bottom-up patterning of polymers using photolithography, printing techniques, self-assembly of block copolymers and instability-induced patterning. In each section, we briefly describe a particular patterning technique, the application of such a technique to polymer patterning, and the most promising applications of the polymer-patterned surfaces. As some of the patterning methods have similar applications, for each technique we highlight the applications in which the method is superior to others.

Patterning of surfaces with non-polymeric or polymer–inorganic materials is beyond the scope of this review. We have not included the

discussion of patterning by layer-by-layer polyelectrolyte deposition, or the fabrication of 3D patterns using multiphoton irradiation. These topics have been covered in depth in several other reviews<sup>13–15</sup>. We also focus on the use of light-based patterning in the fabrication of LEDs, and direct the reader to excellent reviews on the progress in organic electronics and optoelectronics<sup>3,16,17</sup>.

## PHOTOLITHOGRAPHY

Over the past three decades, photolithography has been one of the main methods used for the patterning of polymers. In photolithographic methods, patterns are generated by selectively exposing a monomer-, oligomer- or polymer-coated surface to photoirradiation, and, when needed, by subsequently removing selected areas of the film through dissolution in an appropriate solvent (Fig. 1a). Irradiation triggers photopolymerization, photocrosslinking, functionalization and decomposition reactions, or induces phase separation in the exposed areas. Photolithographic patterns can be generated in polymer films and in monolayers, for example, in polymer brushes<sup>16</sup>. Site-specific exposure is achieved by illuminating the film through a mask or by using optical interference (holographic) techniques<sup>15</sup>. The interference methods generate periodic patterns such as Bravais lattices<sup>10,15,18</sup>.

Photolithography is a cost-effective high-throughput technique that is suitable for large-area surface patterning with good alignment, controlled topography and a broad range of features. The resolution of patterns varies from micrometres to sub-100 nanometres. High-resolution patterning is achieved by using non-conventional masks<sup>7</sup>, new photoactive polymers<sup>19</sup>, irradiation at short wavelengths<sup>20</sup> and advanced lithographic optical techniques and set-ups<sup>20</sup>.

Photolithographically patterned surfaces are used in their own right or as templates for subsequent patterning of surfaces with other functional materials. In addition to their traditional use in the semiconductor industry, patterned polymers have found applications in the production of LEDs<sup>21</sup>, polymer-dispersed liquid-crystal displays<sup>22</sup>, photonic crystals<sup>10</sup>, optical components<sup>23</sup>, microarrays of cells and proteins<sup>24,25</sup>, sensors and actuators<sup>26</sup> and devices for data storage<sup>27</sup>.

Photolithographic patterning of conductive polymers, such as polyacetylene, poly(*p*-phenylenevinylene), polyaniline and

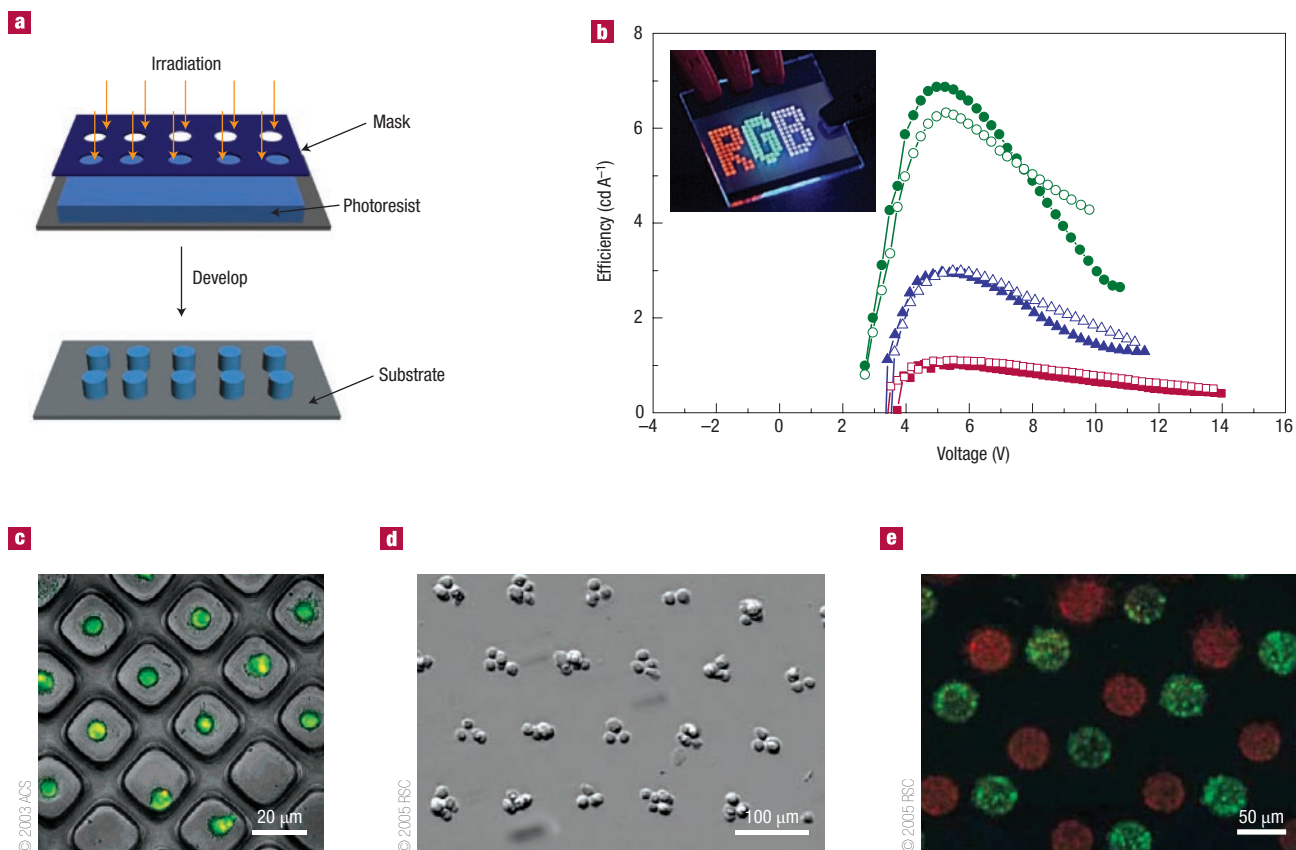


**Figure 1** Patterning of polymers by photolithography. **a**, Schematic of the photolithography technique. **b**, The luminous efficiency for red-emitting (squares), green-emitting (circles), and blue-emitting (triangles) devices. Reproduced with permission from ref. 21. The open symbols refer to the crosslinked devices and the filled symbols to the non-crosslinked reference devices. Inset is a photograph of an RGB (red, green, blue) device. **c**, Confocal microscopy image of 3T3 fibroblasts confined within PEG microwells with  $30 \times 30 \mu\text{m}$  individual dimensions. Reproduced with permission from ref. 24. **d**, Bright-field microscopy image of fibroblast clusters arrayed within PEGDA hydrogel. **e**, Fluorescence microscopy image of two types of dye-labelled cells encapsulated within PEGDA domains on a hydrogel layer. Reproduced with permission from ref. 32.

polythiophene, is a growing field of research in the development of LEDs<sup>21,28</sup>. Figure 1b shows a three-colour display fabricated from three oxetane-functionalized, electroluminescent spirobifluorene-*co*-fluorene polymers individually emitting blue, green and red light<sup>21</sup>. Patterning was achieved by photocrosslinking soluble polymers to generate insoluble polymer networks in the desired areas. The patterned polymers retained their electrical and optical properties, and the device showed efficiencies comparable to state-of-the-art organic LEDs. Patterning of light-emitting polymers was also achieved by the photo-crosslinking of light-emitting monomers and oligomers. For example, a full-colour LED was fabricated by selective photoinitiated crosslinking of liquid-crystalline light-emitting oligomers<sup>28</sup>. Owing to the photo-alignment effect, the device showed a significant improvement in photoluminescence quantum efficiency and hole mobility, compared with the non-patterned oligomeric liquid crystals<sup>28</sup>.

Biologically, photolithographically generated polymer patterns have enabled the precise manipulation and localization of cells and control of cell–cell and cell–substrate interactions. Patterning includes site-specific formation of islands for cell seeding<sup>24,29–31</sup> or photochemically crosslinked hydrogels that encapsulate cells<sup>25,32</sup>. In comparison with other patterning techniques, photolithography provides geometric confinement of cells in addition to lateral compositional patterns for cell adhesion. The combination of

these features suppresses time-dependent deterioration of cell arrays. Examples of polymers used for cell patterning included synthetic hydrogels (for example, poly(ethylene glycol)<sup>25,32</sup> or poly-*N*-isopropylacrylamide<sup>29</sup>), biological hydrogels (for example, chitosan<sup>30</sup>), and biohybrid hydrogels such as a PEG-based hydrogel modified with peptide Arg–Gly–Asp (RGD)<sup>24,31</sup>.

Figure 1c shows a planar array of 3T3 fibroblasts, in which individual cells are confined in PEG hydrogel wells<sup>24</sup>. The cell occupancy within the well was 96.7%, and the cells remained viable for 24 hours. Encapsulation of living cells allowed mimicry of the cell's microenvironment *in vivo*<sup>25,32,33</sup>. Precise positioning of cells in a solution of poly(ethylene glycol) diacrylate (PEGDA) and polymer photocrosslinking yielded more than 20,000 cell clusters with cell viability of more than two weeks (Fig. 1d)<sup>32</sup>. Multistep photoirradiation enabled the patterning of several distinct cell types within the same segment of hydrogel (Fig. 1e). By modulating cell–cell interaction in 3D, the first evidence was presented that microscale tissue organization regulates the biosynthesis of bovine articular chondrocyte<sup>33</sup>.

Holographic methods have been proven successful in the fabrication of polymer-dispersed liquid crystals (PDLCs)<sup>34</sup>, and 3D photonic crystals<sup>10,15,18</sup>. Holographic PDLCs have applications such as reflective flat-panel displays, switchable lenses and optical switches<sup>34,35</sup>. Patterning of PDLCs is achieved during photopolymerization, owing to the anisotropic diffusion and phase separation of liquid crystals in

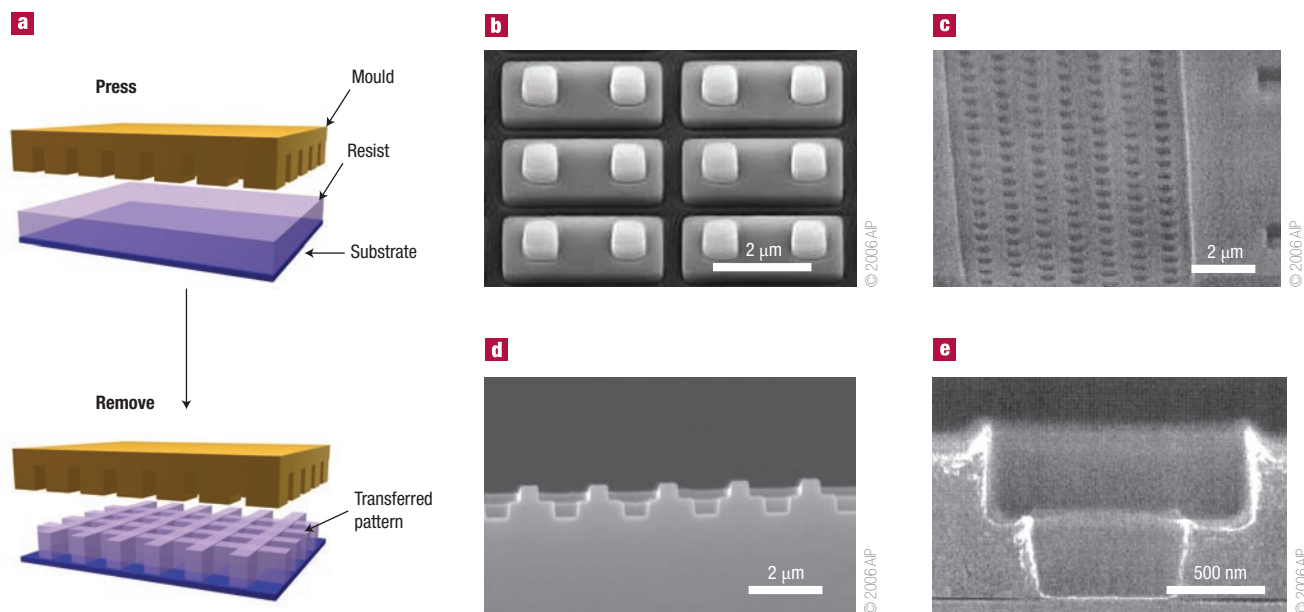


**Figure 2** The nanoimprinting technique. **a**, Schematic of polymer patterning. **b**, SEM image of multi-tier template. **c–e**, SEM images of top-view (**c**), cross-sectional view (**d**), and a close-up of an individual component of the polysilsesquioxane structure patterned by nanoimprinting (**e**). Reproduced with permission from ref. 53.

polymerizable precursors. Liquid crystals segregate into nanoscopic domains at the null points of the interference pattern, producing arrays of droplets dispersed in polymers<sup>35</sup>. In holographic patterning, photoresists should not strongly absorb or scatter light in the spectral range of the irradiation whereas photopolymerization should not perturb the interference pattern on the timescale of the irradiation<sup>10</sup>. These requirements are addressed by implementing new optical designs of holographic set-ups and developing new photoresists<sup>36,37</sup>. Furthermore, multiple exposure and the use of fewer laser beams enables the simplification of optical set-ups and the diversification of the structures that are produced by holography<sup>18,38</sup>. Patterning by interference holography is simpler and more efficient than direct laser writing by multiphoton polymerization<sup>14</sup>; however, it is less flexible, owing to the generation of only specific types of patterns.

Overall, two major challenges in photolithography are to continuously enhance low-cost high-resolution patterning; and to pattern functional polymers without compromising their properties. For example, owing to the weak bonds present in  $\pi$ -conjugated polymers, direct photoirradiation causes polymer degradation (for example, photo-oxidation) and the deterioration of its electronic and optical properties. The functionalization of conductive polymers with crosslinkable reactive groups<sup>21</sup> or photothermally induced patterning helps to preserve polymer properties<sup>39</sup>. Although prototype devices have been made from model conjugated polymers, imparting patterning and function to commercially feasible polymers has not yet been accomplished. Currently, cost-effective printing techniques can successfully compete with photolithographic methods for the patterning of conductive polymers, especially in patterning mass-produced components.

Photolithography is not suitable for the direct patterning of bioactive species with a high sensitivity to UV-irradiation, photoinitiators and solvents used for the development of patterns. The method is also not suitable for the patterning of curved surfaces. In addition, patterning with high resolution is usually achieved at higher cost; thus, other techniques derived from photolithography (for example, soft-lithography) prove to be a useful alternative for the fabrication of chemical and topological structures.

## PRINTING TECHNIQUES

Modern printing methods for polymer patterning include conventional printing techniques such as xerography and ink-jet, screen, offset and intaglio printing, and relatively new methods such as dip-pen lithography, nanoimprinting, microcontact printing, and robotic deposition. Printing methods can be tentatively classified into two groups: techniques involving the contact of a stamp or a writing head with a substrate, and the methods in which an 'ink' material is transferred to the substrate without direct contact with the surface.

### NANOIMPRINTING

In nanoimprint lithography (NIL) the patterning of polymers is realized by pressing a mould against a softened thermoplastic polymer or a liquid polymer precursor and trapping the pattern in the solid state by either cooling the moulded material (thermal NIL), or by UV-photocuring the polymer precursor (UV-NIL), as shown in Fig. 2a. The soft material is driven into the recessed portions of the mould by applied pressure, adhesion or capillarity. The materials to be patterned can be spun-cast, dispensed as droplets, or allowed to fill the space between the mould and substrate by capillary forces. After embossing, the resulting pattern can be further processed to etch away the thin regions of the pattern, to etch the exposed substrate material, or to selectively deposit other materials<sup>16</sup>. Both thermal NIL and UV-NIL methods have demonstrated as low as 5-nm horizontal patterning resolution<sup>40,41</sup>, yet UV-NIL requires lower imprinting pressures, shorter patterning times, and simpler fabrication of multilevel topographic patterns. For an overview of method-related and materials-related developments in NIL the reader is referred to other review articles<sup>16,42,43</sup>.

A wide range of thermoplastic polymers, including poly(methyl methacrylate) (PMMA), polystyrene (PS), polycarbonate, and poly(vinyl alcohol) are being used for thermal NIL at patterning temperatures exceeding the polymer glass-transition temperature. Commercial photoresists patterned with thermal NIL serve as pattern-transfer masking layers in subsequent photolithographic patterning<sup>44</sup>. More sophisticated polymer systems include conducting

polymers<sup>45</sup>, polymers labelled with fluorescent chromophores<sup>46</sup>, and block copolymers<sup>47</sup>. Thermosetting polymers<sup>48</sup> and solvent-containing hydrogen silsesquioxane or tetraethoxysilane compounds<sup>49</sup> have also been used for thermal NIL. The challenge in thermal NIL is the difficulty in the patterning of highly viscous polymers. Topographic patterns imprinted in thermoplastics have found applications in the fabrication of low-*k* dielectric materials, optical components (for example, light couplers, filters for waveguides, lasers and 2D photonic crystals), pattern-transfer masks, compact disks and digital video discs.

In contrast with thermal nanoimprinting lithography, UV-NIL uses photosensitive polymer precursors with high curing rates and intermediate viscosities. The use of low-viscosity precursors is usually limited, owing to the evaporation of the material before patterning is completed. Photocuring is realized by free-radical or cationic polymerization, however, because of the longer lifetime of cationic catalysts and the acidic nature of cationic initiators, UV-NIL is generally achieved by free-radical polymerization. This method is also not free of problems, such as sensitivity to oxygen and polymer shrinkage that can be as high as 10%<sup>50</sup>. Oxygen inhibition can lead to defects in high-resolution patterns: uncured material at the mould edge can generate particles. This problem can be resolved by designing new polymers, for example, oxygen-insensitive thiolene polymers<sup>51</sup>. A study of shrinkage-induced stress in UV-NIL-patterned surfaces is an area of ongoing research activity: stress can be potentially beneficial for mould release but it can also reduce mould lifetimes<sup>43</sup>. Potential approaches to reduced shrinkage include the use of ring-opening polymerization and the inclusion of bulky pendants in the precursor molecules.

Recently, sophisticated chemistries were introduced for NIL-patterning to fabricate semiconductor, electronic, nonlinear optical and microfluidic devices, and the substrates for cell and bacterial growth. Photocurable teflon-like materials were used for the fabrication of solvent-resistant microfluidic devices<sup>52</sup>. UV-NIL of photocurable precursors to conductive polymers demonstrated applications in the direct patterning of electronic circuits<sup>45</sup>. Dielectric materials, for example, polyhedral 'cage-like' oligomeric silsesquioxanes functionalized with photocuring groups were patterned by multi-tier imprint moulds<sup>53</sup>. As an example, Fig. 2b–e shows a multi-tier template and a corresponding multilevel imprint patterned in a single step in the photocurable polyhedral silsesquioxane derivative<sup>53</sup>. We note that the fabrication of similar multi-tier structures by means of conventional photolithography would require the use of multiple photoresist layers and several exposure steps<sup>54</sup>.

Nanoimprint lithography is a competitive method for the patterning of polymers. Careful control of mould geometries and process parameters yields highly reproducible patterns. Commercial nanoimprinting tools are already available for academic and industrial purposes. Future applications for nanoimprinting depend on the development of new photochemically sensitive materials that are not susceptible to oxygen inhibition, not prone to shrinkage, and are easily removed from moulds with high aspect ratios.

#### MICROCONTACT PRINTING

Microcontact printing ( $\mu$ CP) is an efficient technique for the patterning of large-area surfaces with spatial resolution down to the submicrometre range<sup>55</sup>. In  $\mu$ CP, a rigid or elastic stamp with bas relief features is used to transfer an 'inked' material to the substrate (Fig. 3a). The conformal contact between the substrate and the raised regions of the stamp provides high fidelity when transferring an 'ink' to the surface<sup>55,56</sup>. High-quality  $\mu$ CP patterns are generated under optimized conditions that avoid contamination, the deformation of stamps and the lateral diffusion of the ink<sup>57–59</sup>. For more details on the  $\mu$ CP patterning the reader is referred to two excellent reviews<sup>60,61</sup>.

Soon after the invention of  $\mu$ CP<sup>55</sup>, the method became extremely useful in the direct and indirect patterning of surfaces with polymer monolayers and thin films. In direct  $\mu$ CP, a stamp carrying a polymer solution transfers the polymer to the surface. High-resolution patterning is not easily realized because of the large size of macromolecules and/or multivalency of macromolecules. In indirect  $\mu$ CP, selective deposition of a polymer or a monomer to the pre-patterned surface is followed by the surface-initiated polymerization, site-specific electropolymerization, layer-by-layer deposition of polymers, or back-filling<sup>62–64</sup>.

To achieve high-resolution patterning, the deterioration of surface features by lateral diffusion is suppressed by using polymers that strongly interact with the surface. For example, electrostatic interactions between cationic poly(acrylic acid) and cationic poly(allylamine hydrochloride)-coated substrate enabled patterning with a resolution of 80 nm (ref. 65; Fig. 3b). High-fidelity patterns can also be realized in reactive  $\mu$ CP (ref. 66). For instance, patterning of poly(ethylene imine) on surfaces coated with monolayers comprising carboxylic anhydride groups generated structures with edge resolution of 500 nm (ref. 66). Alternatively, small 'heavy-weight' macromolecules such as dendrimers are suitable for high-resolution patterning: surface features with sizes below 50 nm were realized in patterns of polyamidoamine G4 dendrimer, owing to the suppressed lateral diffusion of polymer molecules<sup>56</sup>.

In indirect  $\mu$ CP, atom-transfer radical polymerization was used to pattern surfaces with 5–50-nm-thick layers of polymer brushes of polyacrylates<sup>62</sup>. Site-specific polymerization was accomplished by anchoring an initiator to the pre-patterned surface. The surface density of brushes was higher than in most existing 'grafting to' approaches in which the excluded volume effects limited the density of grafting<sup>62</sup>. Surface-initiated polymerization on pre-patterned surfaces has also enabled the patterning of binary, tertiary and quaternary polymer brushes<sup>67</sup> as shown in Fig. 3c.

Microcontact printing is suitable for reel-to-reel or sheet-to-sheet production schemes, and it does not need clean rooms or expensive optical instrumentation. The past decade has seen tremendous progress in the applications of  $\mu$ CP methods in the field of organic electronics<sup>16</sup>, namely, in the production of organic LEDs, thin-film transistors, electronic paper, integrated circuits and microoptical parts. Organic thin-film transistors with electrodes fabricated from conductive polymers showed excellent electrical performance of 0.7 cm<sup>2</sup> V<sup>-1</sup> S<sup>-1</sup> field-effect mobility and the on–off current ratio on the order of 10<sup>6</sup> in the saturation regime, due to the low energy barriers for hole carrier injection of patterned electrodes<sup>68</sup>.

Microarrays of synthetic and natural polymers patterned by  $\mu$ CP have been used to enable precise control of cell adhesion and the immobilization of biological molecules on various substrates. Site-specific immobilization of proteins, NIH3T3 fibroblasts, or microvascular endothelial cells was achieved by selectively coating the surface with poly(oligoethyleneglycol methacrylate)-based polymer thus creating protein-resistant areas<sup>69,70</sup>. Figure 3d shows cells grown on cell-adhesive fibronectin islands surrounded with cell-resistant PEG-covered areas<sup>5</sup>. The anisotropic cell-adhesive micropatterns controlled the spatial distribution of the extracellular matrix secreted by individual cells, and thus guided the compartmentalization of cells and the orientation of cell polarity<sup>4,5</sup>.

The  $\mu$ CP technique has already triggered enormous developments in plastic electronics, optics, surface sciences and biorelated fields. In the future,  $\mu$ CP will continue to have an important role in polymer patterning, especially in combination with other patterning techniques such as photolithography, dip-pen lithography or the self-assembly of block copolymers. In spite of its merits, the technique has limitations, for example, the difficulty in the production of multilayer and multicomponent patterns. Although patterning with sub-100-nm resolution is feasible, most of the routinely generated  $\mu$ CP patterns have features in the micrometre size range.

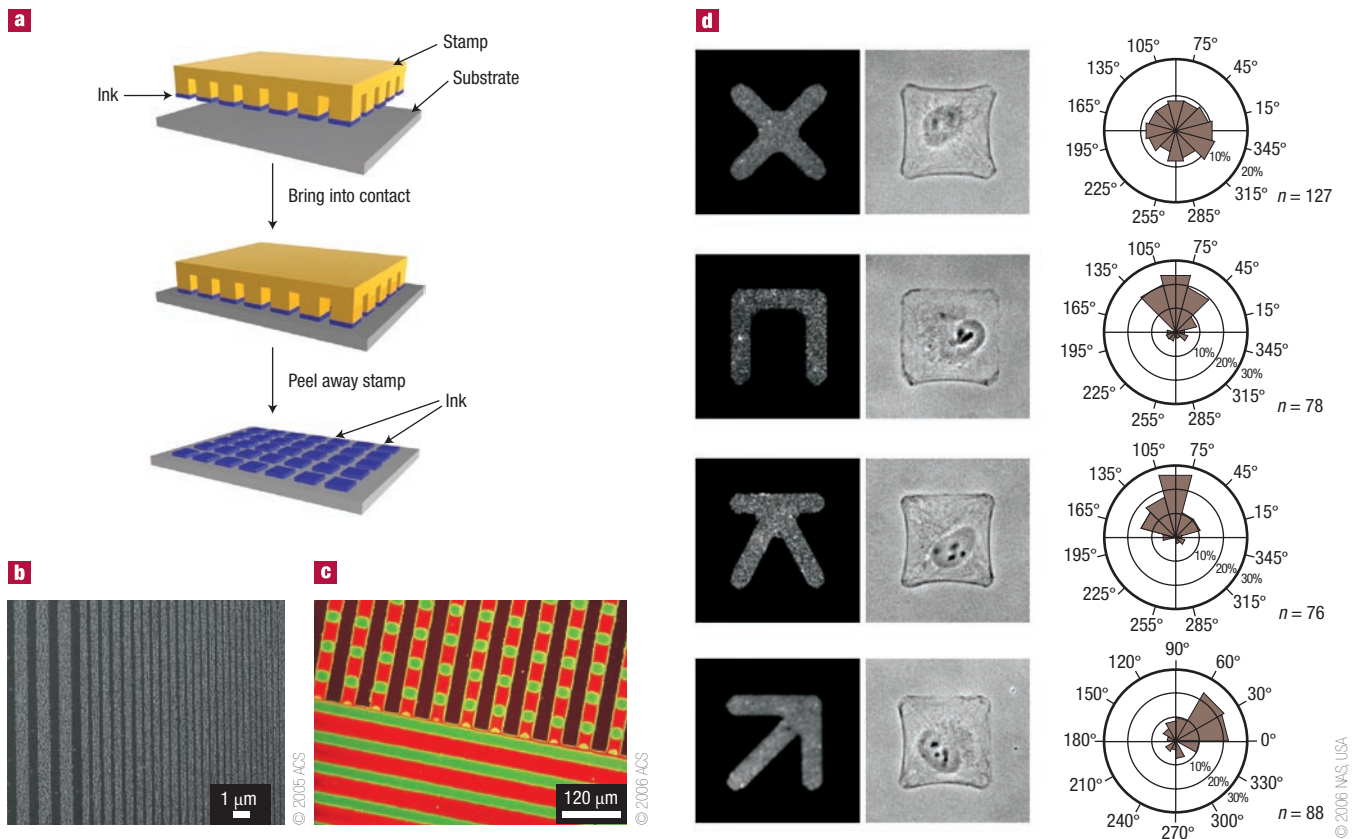


**Figure 3** Microcontact printing. **a**, Schematic of polymer patterning. **b**, Images of 96-nm polystyrene beads deposited on the lines of patterned polyelectrolyte complexes. Reproduced with permission from ref. 65. **c**, Fluorescence image of patterned tertiary brush of acridine-stained poly(methacrylic acid) (dark area) / poly(methacryloylethylphosphate) (bright red area) / poly(*N*-isopropylacrylamide) (green area). Reproduced with permission from ref. 67. **d**, Dependence of cell orientation on fibronectin adhesive pattern surrounded with PEG (left); phase-contrast microscopy of RPE1 cells plated on fibronectin micropatterns with similar square convex envelopes (middle); distribution of cell polarity axis (right). On the X-shape pattern, cells displayed random orientation, on other patterns, the cell polarity axis was oriented toward the adhesive edges. In **(d)** the size of micropatterns is  $33.5 \times 33.5 \mu\text{m}^2$ . Reproduced with permission from ref. 5.

#### DIRECT WRITING TECHNIQUES

Patterning by direct writing is realized by delivering chemical reagents from a nozzle or from a probe tip to specific regions of the substrate. Pattern geometry is defined by the computer-controlled motion of the nozzle or the tip along the surface. Here, we divide direct writing techniques into two groups: (1) the scanning probe microscopy-based methods and (2) the ejecting methods such as ink-jet printing and robotic deposition.

In scanning probe microscope lithography the tip of an atomic force microscope (AFM) or a scanning tunnelling microscope selectively covers the underlying substrate with the patterning material (constructive patterning), or removes and modifies the underlying substrate by applying mechanical force, heating, or an electric field (destructive patterning)<sup>61,71</sup>. Sometimes, the patterning material is subsequently deposited onto the pre-patterned surface. The scanning probe microscopy methods allow for both extremely high (down to several nanometres) resolution patterning and *in situ* imaging of the resulting patterns<sup>71</sup>.

Dip-pen nanolithography (DPN) is a relatively new, 'constructive' technique, which appeared soon after the demonstration of patterning by conventional scanning probe lithography methods such as nanografting or nanoshaving<sup>71,72</sup>. When an 'ink'-coated AFM tip is translated above the surface, a liquid meniscus forms between the tip and substrate, and the ink molecules transfer from

the tip to the underlying substrate as a result of chemical or physical adsorption of the ink to the surface (Fig. 4a)<sup>72</sup>. For a particular type of ink, the resolution of patterning depends on the scanning speed, the volume of meniscus, the surface chemistry, the temperature and the ambient humidity<sup>72–75</sup>.

Patterning of polymer nanostructures by DPN is accomplished in two ways: by depositing on the surface-reactive precursors and subsequently conducting site-specific polymerization reactions<sup>76</sup>, or by directly delivering to the substrate polymer molecules from their solutions or melts<sup>77–79</sup>. The rate of polymer transfer from the tip to the surface and the size of pattern features strongly depend on the dimensions of the polymer molecules. A study of patterning of starburst polyamidoamine dendrimers (G1–G4) and polypropylene imine dendrimers (G5) showed that the rate of polymer delivery to the substrate and the size of pattern features decreased with increasing molecular mass of the polymers<sup>79</sup>.

Strong polymer–surface interactions provide the driving force for the transfer of polymer molecules from the tip to the surface: negatively charged sulphonated polyaniline and doped polypyrrole transferred from the AFM tip to the oppositely charged substrates, but not to the neutral or positively charged surfaces<sup>78</sup>. To realize strong polymer–surface interactions, polyamidoamine G-5 dendrimers were covalently patterned on reactive *N*-hydroxysuccinimide (NHS)-terminated monolayers and NHS-activated block-copolymer platforms<sup>80</sup>.

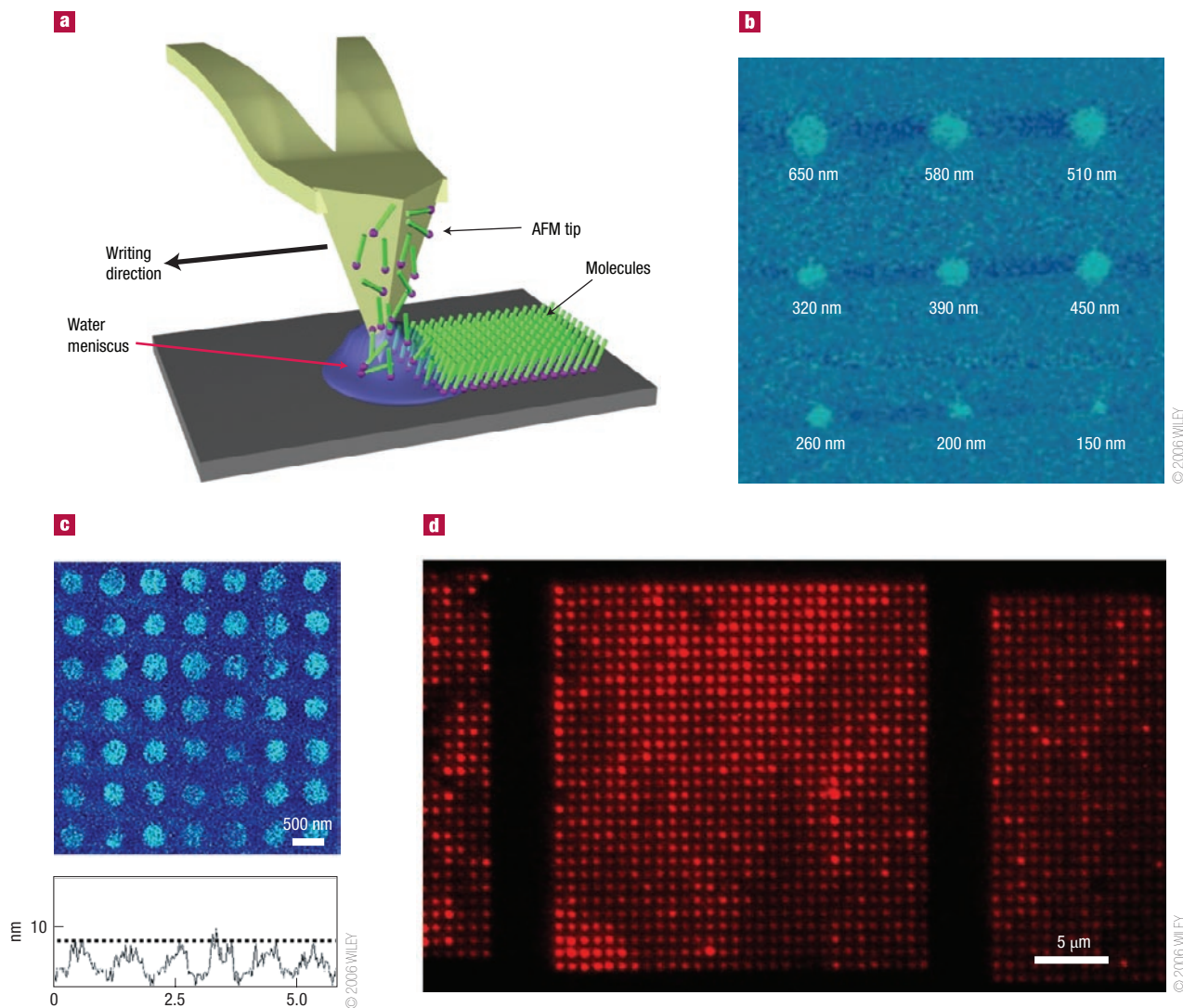


**Figure 4** Dip-pen nanolithography. **a**, Schematic representation of the patterning process. A water meniscus forms between the solid substrate and the AFM tip that is coated with 'ink' molecules. **b**, Phase-tapping-mode AFM images of nine protein A/G dots generated at different contact times between an AFM tip and a gold substrate (650 nm: 8 s, 580 nm: 7 s, 510 nm: 6 s, 450 nm: 5 s, 390 nm: 4 s, 320 nm: 3 s, 260 nm: 2 s, 200 nm: 1 s, 150 nm: 0.5 s). **c**, Topographical tapping mode AFM image and the corresponding height profile of fluorescein isothiocyanate Alexa Fluor 594-labelled human IgG nanoarrays immobilized onto protein A/G templates. **d**, Fluorescence microscopy image of Alexa Fluor 594-labelled antibody nanoarray. The patterns span the distance of 1 cm. Reproduced with permission from ref. 85.

The DPN method has also proven useful in the patterning of molten polymers, for example, poly(3-dodecylthiophene), by using an AFM tip integrated with a heater<sup>77</sup>. The patterning generated multilayers of poly(3-dodecylthiophene) with each layer being aligned along the deposition direction and with the alkyl groups oriented perpendicular to the substrate<sup>77</sup>. The polymers transferred from the tip to the substrate when the temperature of the tip exceeded the melting temperature of the polymer, by contrast with thermomechanical writing developed at IBM<sup>81</sup>.

Patterning of low-molecular-weight precursor molecules, such as pyrrole or caffeic acid, and their subsequent polymerization has been used to create high-resolution patterns<sup>76</sup>. Electrochemical polymerization combined with DPN proved beneficial for the patterning of conducting polymers such as polythiophene and poly(vinylcarbazole)<sup>82</sup>. Lower voltages applied between the AFM tip and the substrate and slower translation speeds yielded patterns with a higher resolution. Recently, the capabilities of DPN were enhanced

by using multiple AFM tips (the 'millipede' technology<sup>83,84</sup>), by using durable tips that carried more ink<sup>73</sup>, and by using individually activated tips<sup>74</sup>.

Patterning by DPN has also been used for the production of arrays of biopolymers<sup>75,85</sup>. Owing to the high density of arrays, reduction of sample volume, and the ability to screen a larger number of targets, micro- and nanoarrays of proteins and DNA show promising applications in fundamental studies of biological recognition and throughput diagnostics. Figure 4b–d shows a nanoarray of protein A/G that on patterning retained its biological selectivity for the study of the molecular binding of human IgG protein<sup>85</sup>. The size of protein dots was reduced by decreasing the contact time between the AFM tip and the substrate (Fig. 4b).

In ink-jet printing, a jet of a polymer solution breaks up into droplets, which are deposited onto a surface, and form a pattern when the solvent evaporates (Fig. 5a). Polymer patterning can also be achieved by depositing onto a polymer substrate droplets of a solvent

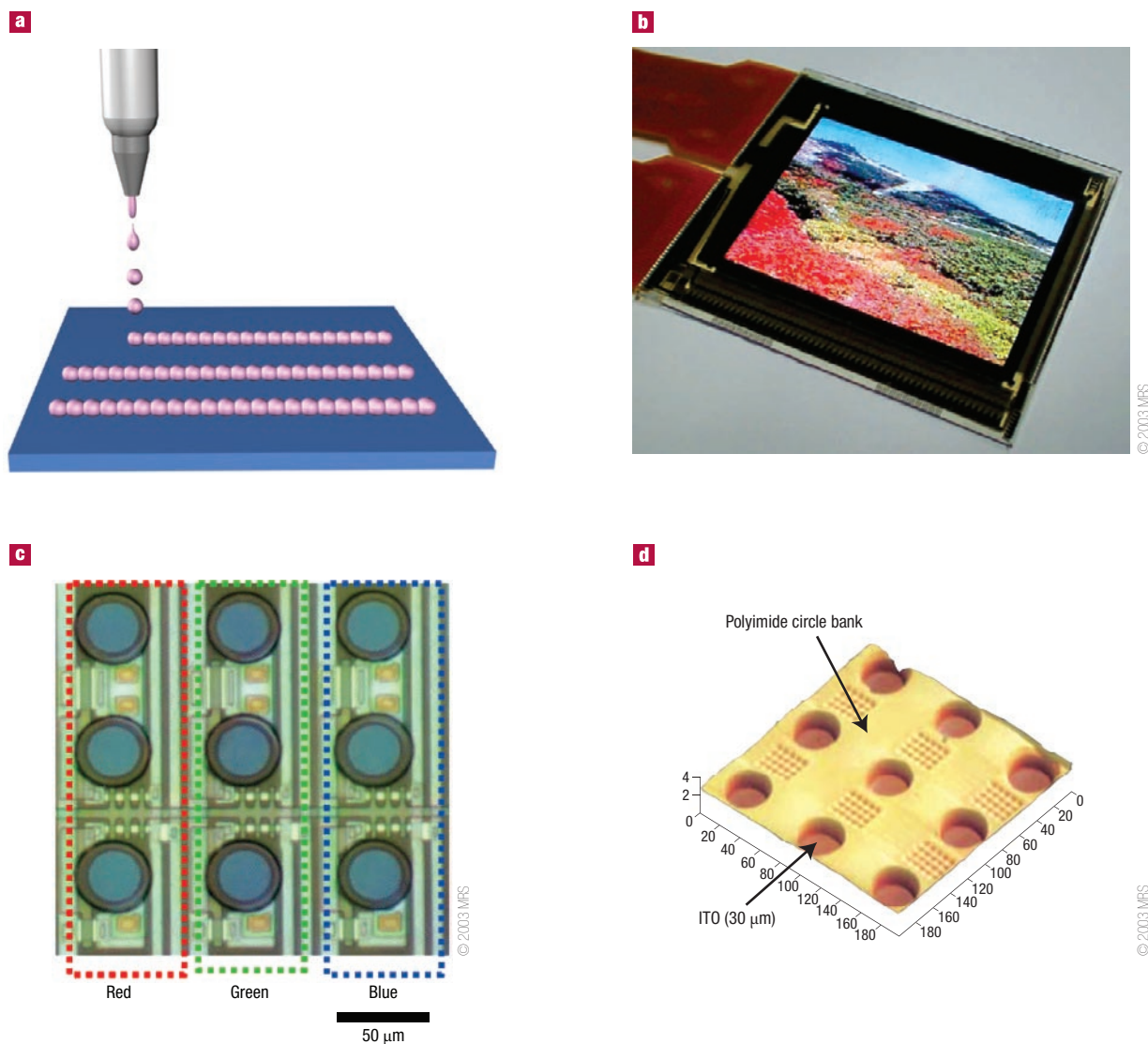


**Figure 5** Inkjet printing. **a**, Schematic of the patterning process. **b**, Picture of the organic electroluminescent display fabricated by inkjet printing. **c**, Colour pixel made up of three columns comprising nine subpixels. **d**, An AFM image of the pixel. 3- $\mu\text{m}$ -deep circular holes of 30  $\mu\text{m}$  diameter through the polyimide circle bank expose ITO (indium tin oxide) on the bottom layer. Reproduced with permission from ref. 1.

or a reactive ink that selectively etches the polymer<sup>86,87</sup>. The smallest size of the droplets determines the resolution of the method (usually on the order of 10  $\mu\text{m}$ ). The size of features can be reduced by using acoustic and electrohydrodynamic ink-jetting, ink-jet printing on pre-patterned surfaces, and self-aligned ink-jet printing<sup>1,86,88,89</sup>.

Ink-jet printing has been used to pattern photoresists, polyelectrolytes, conjugated polymers, biopolymers, photocurable oligomers and monomers, and polymer colloids. Polymer solutions used for patterning should possess well-defined rheological properties, surface tension and solvent volatility<sup>90</sup>. The non-newtonian nature of polymer solutions complicates the break-up of jets: nonlinear effects — for example, strain hardening — occur due to high extensional stresses and suppress the break-up of jets<sup>90</sup>. Viscosity of polymer solutions is controlled by selecting polymers with suitable molecular weights and architectures and by tuning polymer concentration.

Patterning of polymers by ink-jet printing has been used in the fabrication of waveguides, microlens arrays<sup>87</sup>, sensors<sup>91</sup> and arrays of cells and proteins<sup>92</sup>. The technique is entering a mature state in plastic

electronics, for example in the production of polymer transistor circuits and organic LEDs. The challenge in ink-jet printing of electronic devices is to achieve precise, reproducible patterning with resolution less than 10  $\mu\text{m}$ , while preserving polymer crystallinity, anisotropy and stability against dissolution of inner layers in multilayer films.

Ink-jet patterning has enabled the production of polymer transistor circuits<sup>87</sup> and the fabrication of high-performance full-colour LEDs<sup>1</sup>. Figure 5b–d shows a full-colour (RGB) multilayer flexible polymer display produced by ink-jet printing: a close-spaced, well-aligned array of red (R), green (G) and blue (B) pixels of light-emitting polymers<sup>1</sup>. Each pixel contains three sub-pixels corresponding to the individual colours (Fig. 5c). The pixels were obtained by depositing light-emitting polymers on the polyimide film pre-patterned with holes (Fig. 5d). Control of the order in which the solvents and the polymers were deposited on the substrate was required to avoid the dissolution and the swelling of the underlying layers.

In robotic deposition, a filament of an ink material is continuously extruded from a nozzle and is deposited on a substrate to yield 2D or

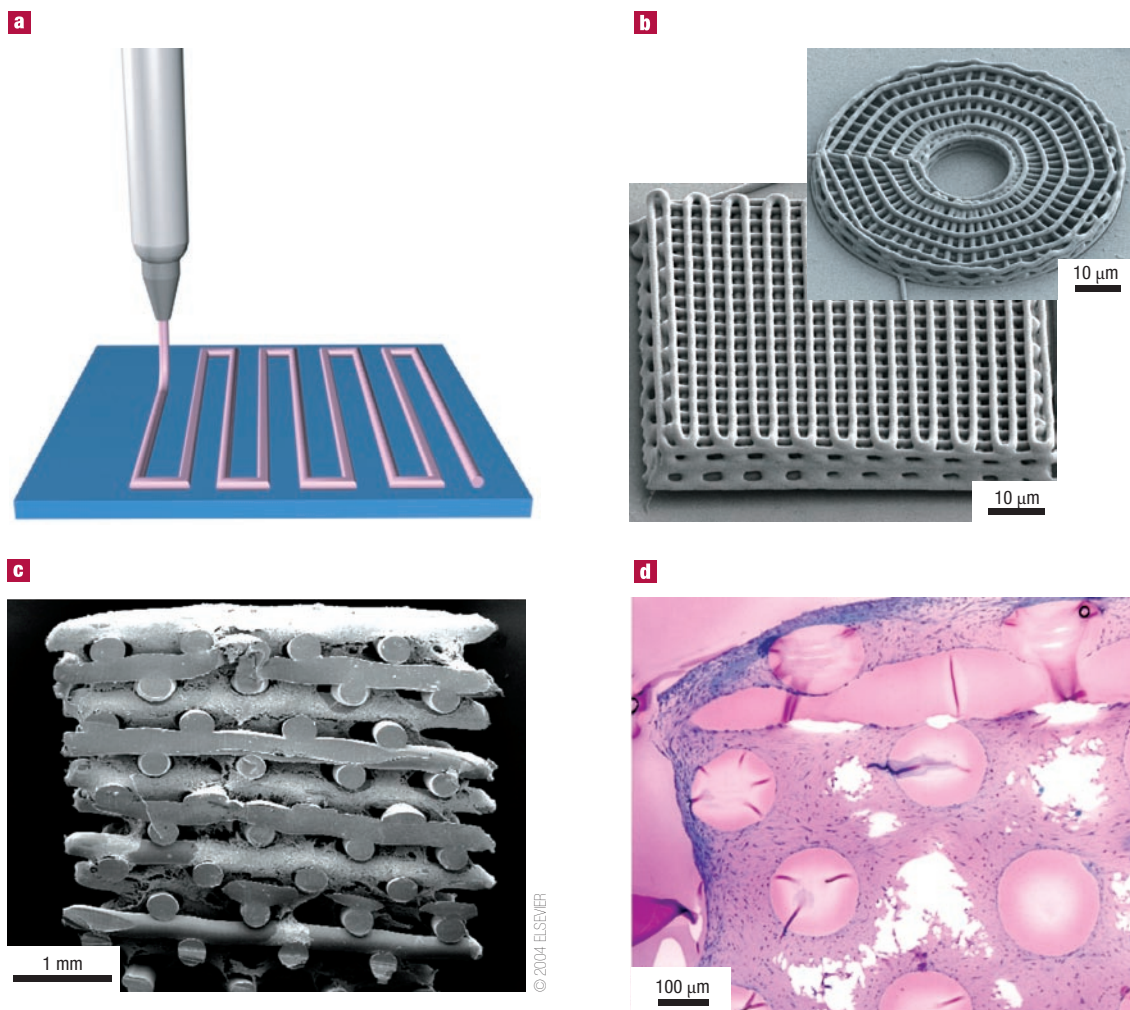


**Figure 6** Robotic deposition. **a**, Schematic of the patterning process. **b**, Three-dimensional periodic structures with a face-centred tetragonal geometry and a radial array generated by robotic deposition of a mixture of polyelectrolytes. Reproduced with permission from ref. 98. **c**, Scanning electron microscope (SEM) image and **d**, safranin-O sections showing attachment, proliferation and high percentage of expanded human articular chondrocytes throughout the interconnected pores on the 3D-deposited scaffolds. Reproduced with permission from ref. 95.

3D patterns (Fig. 6a). Complex 3D architectures can be produced by a computer-aided layer-by-layer sequential build-up process. Robotic deposition has been used for the patterning of melts, solutions, reactive prepolymers, conductive polymers, polyelectrolytes and polymer dispersions. The resolution of the method is on the order of hundreds of nanometres. The patterning process requires the optimization of viscosity and viscoelasticity of the ink and the hardening of the ink after extrusion from the nozzle.

The technique has proven extremely useful for the patterning of biopolymers and biocompatible polymers. Precisely controlled geometries were produced by robotic patterning of poly-L-lactic acid, polycaprolactone<sup>93</sup>, poly(D-L-lactide-co-glycolide)<sup>94</sup>, poly(ethylene glycol terephthalate-*b*-butylene terephthalate)<sup>95</sup>, agarose, gelatin<sup>96</sup>, chitosan<sup>97</sup> and polyelectrolytes<sup>98</sup>. In the latter case, solutions of non-stoichiometric mixtures of a cationic and an anionic polyelectrolyte were extruded from a nozzle, rapidly coagulating in an alcohol-water solution to form self-supporting filaments. Three-dimensional lattices and radial arrays patterned with a resolution of 1 µm are shown<sup>98</sup> in Fig. 6b.

Patterning by robotic deposition offers an efficient approach to polymer patterns with complex 3D architectures that are

not accessible by conventional lithographic methods. The technique provides an alternative to stereolithography, as it does not require polymer photocuring and causes no damage to light-sensitive materials.

Polymer patterns generated by robotic deposition have applications in the production of photonic crystals, microfluidic devices and templates for biomimetic mineralization<sup>99–101</sup>, however, their most promising application is the fabrication of scaffolds for tissue engineering<sup>102</sup>. Polymer templates with a well-defined geometry, porosity, mechanical properties and appropriate biological cues were used for the organization of cells over the length scales that were required for tissue function<sup>6</sup>. Poly(ethylene glycol terephthalate-*b*-butylene terephthalate) scaffolds have been used for the regeneration of cartilage and bone tissues by seeding and culturing bovine articular chondrocytes. The scaffolds provided a homogenous distribution of the cells and supported the formation of the cartilage-like tissue<sup>95</sup>. A study of cell growth on the scaffold fabricated in polycaprolactone and polycaprolactone-hydroxyapatite composites showed that human-bone-marrow-derived osteoprogenitor cells developed along the osteogenic lineage<sup>103</sup>. As an example, Fig. 6c,d shows the attachment and

proliferation of expanded human articular chondrocytes on the scaffolds that led to the filling of pores with high percentage of living cells<sup>95</sup>.

Comparison of printing methods shows that  $\mu$ CP and dip-pen lithography are advantageous in high-resolution patterning; ink-jet and  $\mu$ CP printing are effective in high-throughput large-area patterning, and DPN and ink-jet printing allow easy patterning of multicomponent polymer patterns with good control over feature position. The ultimate technique of choice depends on the selected polymer, the substrate and the intended application.

### PATTERNING OF SURFACES WITH BLOCK COPOLYMERS

Phase segregation in block copolymer (BCP) films provides an efficient approach to ordered topographic and chemical surface patterns with feature sizes of the order of tens of nanometres. Phase separation in BCPs is driven by the positive mixing enthalpy and low mixing entropy of the constituent blocks. Thermodynamically, the structure of BCP films is determined by the molecular weight, composition and architecture of the BCP, and the volume and degree of incompatibility of the constituent blocks (characterized by the Flory–Huggins parameter,  $\chi$ )<sup>104</sup>. Kinetic effects allow additional control over pattern features. The variation in experimental conditions of BCP patterning, for example, different solvent vapour pressure and varying humidity, provide a large parameter space for the control and optimization of patterns targeted to specific applications<sup>105,106</sup>. Variation in chemistry and topography of surfaces offers another strategy in controlling BCP assembly: the structure of patterns on surfaces can be distinct from the bulk morphologies. Several excellent reviews describe the underlying science of phase separation of BCPs<sup>104,107</sup>.

BCP patterns show a high degree of order and symmetry over 10–100 nm length scales, however, achieving large-area defect-free patterns and specific orientation of anisotropic structures is a challenge. Small, preferential interaction of one block with the substrate or incommensurability of film thickness relative to the natural period of the pattern aligns lamellar and cylindrical domains in BCP films parallel to the substrate<sup>107</sup>. A uniform orientation and long-range lateral order of the microdomains is critical in device-related applications, for example, in the fabrication of displays or memory storage devices. Significant progress has been achieved in controlling BCP assembly via a range of strategies: by tuning film thickness and solvent evaporation rate<sup>107,108</sup>, by using topographically and chemically pre-patterned substrates<sup>109–112</sup>, and by applying external triggers such as electric and magnetic fields or shear force<sup>113–115</sup>. As defects and grain boundaries are energetically unfavourable, they have been ‘healed’ by annealing BCP films above the glass-transition temperature of the polymer<sup>116</sup> or by exposing films to solvent vapours<sup>117</sup>. Combining top-down microfabrication methods with bottom-up self-assembly of BCPs enabled the realization of defect-free patterns over tens to hundreds of micrometres in length<sup>110–112</sup>. This strategy was also used to direct the assembly of BCP mixtures into irregular patterns, providing a route to the integration of self-assembled films in electronic devices<sup>112</sup>. Furthermore, the combination of BCP self-assembly with other patterning methods, for example, with photolithography, enabled the fabrication of multi-level ordered structures<sup>118</sup>.

Patterned BCP films can be used in their own right as photonic crystals<sup>9</sup>, optical waveguides<sup>119</sup> and substrates with tunable wetting properties<sup>120</sup>, or as templates for creating polymer patterns, membranes<sup>121</sup> and nanostructured inorganic materials<sup>122</sup>. An emerging application of patterned BCP films is their use as photonic bandgap materials<sup>9,123</sup>. Control over the position of the stop band is achieved by using BCPs with specific molecular weights or by adding homopolymers to the phase formed by respective constituent

blocks<sup>123</sup>. An intrinsically low dielectric constant contrast between the constituent microdomains in BCPs is increased by selectively incorporating metal nanoparticles in the BCP domains, or by selectively removing one of the phases of the film<sup>124,125</sup>. Response to the variation in temperature, humidity or deformation leads to the change in dimensions of the microdomains and allows for the tuning of the photonic band. For example, a thermoresponsive bandgap switching was achieved by using the complex of poly(styrene-*b*-4-vinylpyridinium methanesulphonate) and 3-*n*-pentadecyl phenol<sup>9</sup>. The shift in the spectral position of the bandgap occurred due to the change in the period of the lamellar structure on heating and cooling, resulting from the reversible hydrogen bonding<sup>9</sup>. Currently, the need to increase lattice periodicity and refractive index contrast, as well as improve the slow response time of BCPs to the change in ambient conditions, makes BCP photonic crystals inferior to more advanced and less demanding methods used for the fabrication of photonic bandgap materials.

Fabrication of nanoporous films is one of the most developed applications of patterned BCP films. Pores form when one of the phases is selectively removed from the BCP film. The removal is achieved by ozonolysis<sup>126</sup>, chemical and/or reactive-ion etching<sup>127</sup>, or by UV-irradiation<sup>128</sup>. For instance, PMMA domains in the poly(styrene-*b*-MMA) BCP were removed by using UV-irradiation of the film<sup>128</sup>, whereas reactive-ion etching of the poly(styrene-*b*-ferrocenyldimethylsilane) film oxidized and removed PS domains<sup>127</sup>. Alternatively, nanochannels were produced by swelling-induced re-construction of poly(styrene-*b*-MMA) films in a selective solvent<sup>129</sup>. Nanoporous films have applications in producing membranes<sup>121</sup>, masks<sup>7</sup>, low-*k* materials<sup>126</sup>, media for catalytic reactions<sup>130</sup> and templates for the patterning or growth of inorganic nanostructures<sup>2,122,128,131–134</sup>. Although reducing the cost of high-resolution (<50 nm) patterning in conventional lithography remains a challenge, the use of patterned BCP films as photoresists seems to be an attractive alternative method<sup>2,7,128,131,133</sup>. Porous BCP films have been used for the fabrication of periodic arrays of nanodomains of elastomers<sup>135</sup>, metals<sup>122</sup> and semiconductors<sup>7,128,131</sup>. In particular, BCP lithography paved the way to the production of dense ( $\sim 10^{11}$  cm<sup>-2</sup>) periodic arrays of holes, dots and wires with small feature sizes (<20 nm) on semiconductor substrates<sup>2,7,128,131,132</sup>. This strategy is compatible with conventional semiconductor technologies and it has attractive applications in the fabrication of semiconductor devices<sup>2,132</sup>. Figure 7a illustrates the process of the fabrication of metal-oxide-semiconductor (MOS) capacitors with increased charge-storage capacity<sup>132</sup>. The device was fabricated by using a nanoporous poly(styrene-*b*-MMA) film as a mask for the etching of SiO<sub>2</sub> substrate and thereby creating a template (Fig. 7b) for further patterning of the silicon electrode (Fig. 7c). After removing the BCP and SiO<sub>2</sub> layers from the surface, a new thin SiO<sub>2</sub> layer was grown on the topographically patterned silicon substrate. This step was followed by the subsequent deposition of tantalum nitride onto the SiO<sub>2</sub> layer. The resulting capacitor shown in Fig. 7d had more than 400% higher charge-storage capacity than an analogous capacitor formed on the smooth silicon surface, although this increase was accompanied by the increased leakage current per lateral device area (Fig. 7e).

Patterned BCP films can be directly used for the site-specific synthesis or sequestering of inorganic nanoparticles and the fabrication of periodic nanostructures<sup>8,134,136,137</sup>. Microdomains in patterned BCP films have served as hosts for nanoparticle precursors and subsequent chemical transformation of the sequestered ions into nanoparticles<sup>8,137</sup>. For example, lead ions that were selectively uptaken by acid-containing domains of poly(methyltetracyclododecene-*b*-2-norbornene-5,6-dicarboxylic acid) films, reacted with H<sub>2</sub>S to generate PbS nanoclusters<sup>8</sup>. Second, self-assembly of inorganic BCPs, for example, poly(styrene-*b*-ferrocenyldimethylsilane) accompanied with subsequent BCP pyrolysis

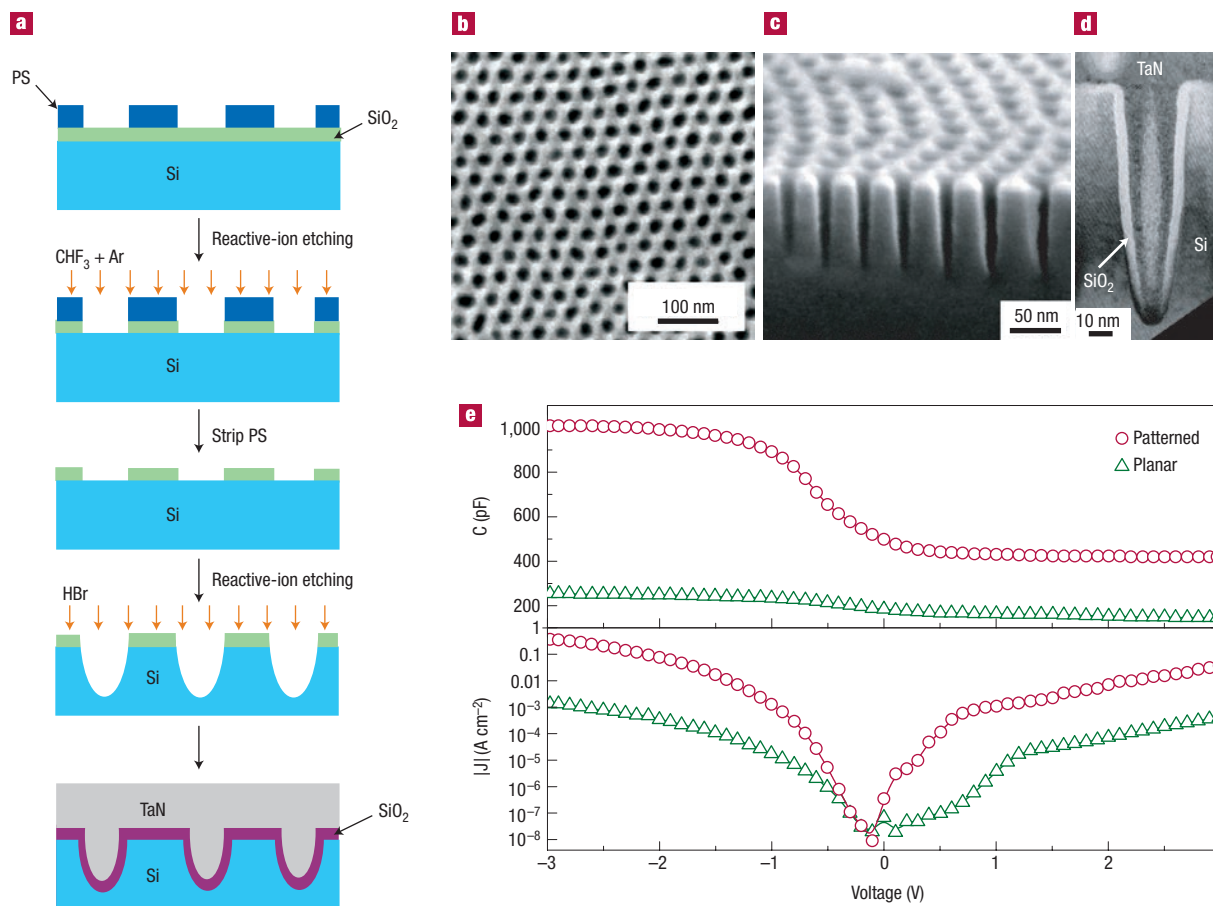


**Figure 7** Patterning of surfaces using the self-assembly of block copolymers. **a**, Processing of the fabrication of a metal-oxide–semiconductor capacitor. **b**, SEM image of the porous template produced by etching a  $\text{SiO}_2$  film through the nanoporous BCP film. **c**, SEM image of the patterned Si electrode. **d**, Transmission electron microscope image of the cross-section of the metal-oxide–semiconductor decoupled capacitor. **e**, Variation in capacitance (upper chart) and leakage current per lateral device area (lower chart) plotted as a function of voltage for planar and patterned devices. Reproduced with permission from ref. 132.

yielded a periodic array of magnetic  $\alpha$ -Fe nanoparticles<sup>136</sup>. In contrast, pre-formed inorganic nanoparticles have been selectively incorporated into one of the phases of the BCP film<sup>138,139</sup>.

### INSTABILITY-INDUCED POLYMER PATTERNING

Subjection of thin, liquid films to vertical temperature or electric field gradients produces modulations in surface tension, buoyancy or charge density<sup>140</sup>. Above the threshold of instability, the system generates a great wealth of lateral spatio-temporal ordered patterns that include hexagons, rings, rolls, spirals and squares<sup>140</sup>. In contrast with simple liquids in which these patterns dissipate after the removal of external field, dynamic structures generated in liquid polymers or monomers can be vitrified by reducing the temperature, evaporating a solvent or polymerizing a polymer precursor, yielding large-scale periodic chemical or topographic patterns<sup>141–144</sup>.

Surface-tension-driven or buoyancy-driven convection patterns were generated in films of liquid monomers subjected to vertical temperature gradients<sup>141–144</sup>. When the Marangoni or Rayleigh numbers exceeded the threshold values characteristic for the onset of instability, the system underwent convection, producing hexagonal or ring patterns with periodicity varying from hundreds of nanometres to several millimetres. The patterns were preserved in the solid state by photoinitiated polymerization of the monomer<sup>143,144</sup>. Convection

patterns have also been used as a template to induce convection in a liquid layer of the convection-passive monomer that was brought in contact with the template layer. Polymerization of the monomer yielded highly ordered hexagonal topographic patterns<sup>142</sup>.

Evaporation of solvents from thin films of binary and ternary polymer solutions generates vertical temperature gradients in the films, and makes them susceptible to Bénard–Marangoni convection<sup>140,141,145</sup>. Phase separation and vitrification ‘freeze’ convection patterns and produce hexagonal compositional and topographic patterns in solidified polymer films. Figure 8a,b shows patterns in films obtained from binary and ternary polymer solutions, respectively<sup>141,143–145</sup>. Patterns generated in thin layers of polystyrene solution in benzene featured a periodic array of holes in the polymer matrix<sup>145</sup> (Fig. 8a). Formation of holes was explained by the condensation of water on the spots with lowered temperature and settling of water droplets, owing to the difference in density with polymer solution. Films obtained from PS–PMMA–toluene solutions featured a hexagonal array of PMMA inclusions periodically embedded in the polystyrene matrix<sup>141</sup> (Fig. 8b).

Currently, polymer patterns generated by surface-tension-driven or buoyancy-driven instabilities are used in fundamental studies of convection in complex fluids. Research is focused on the prediction of periodicity patterns as a function of temperature gradients and macroscopic properties of liquids. To date, it is not clear why

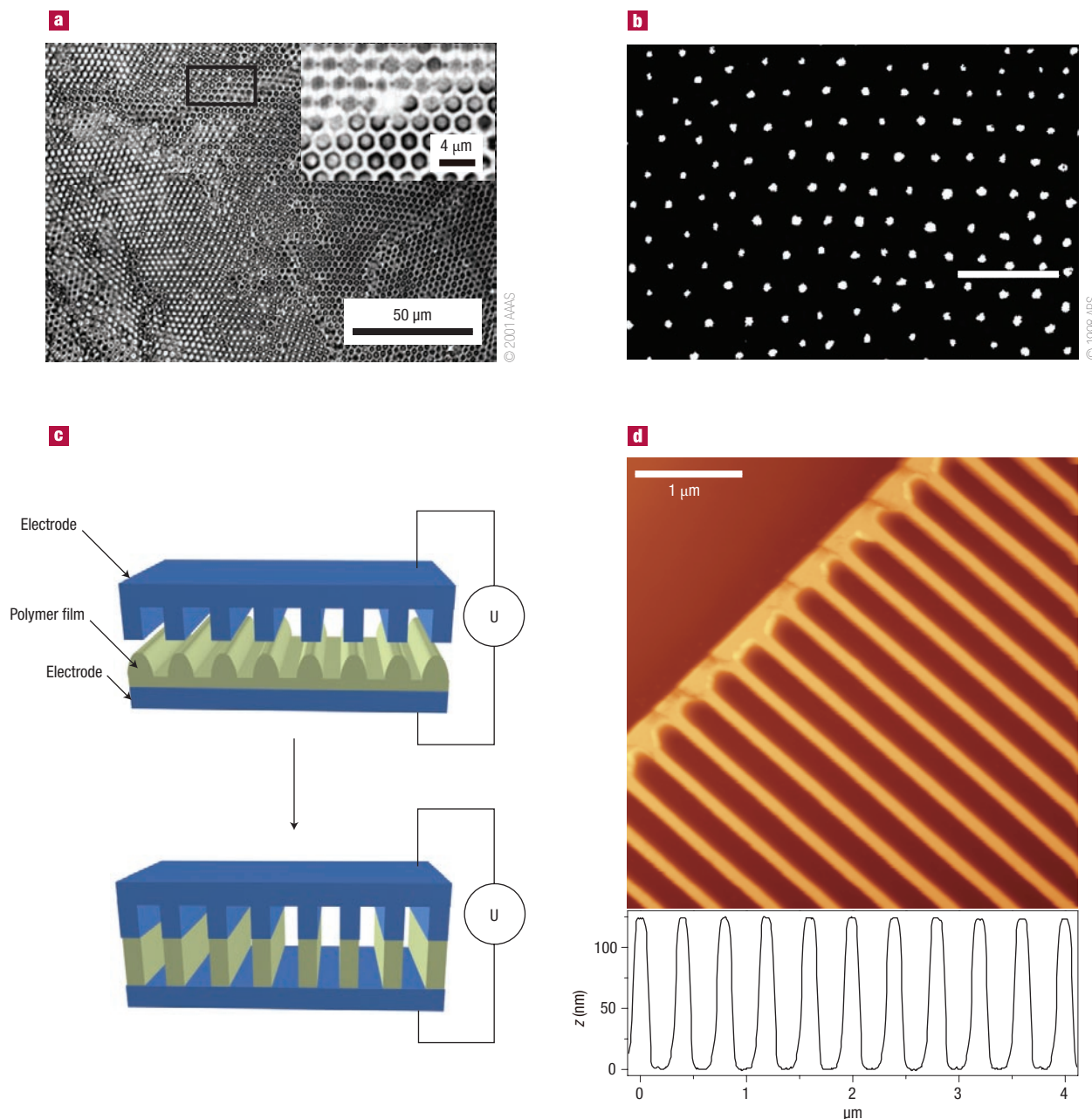


**Figure 8** Instability-induced polymer patterning. **a**, Transmitted bright-field microscope image of polystyrene film with hexagonally ordered array of holes, which are obtained due to thermocapillary convection in thin films of PS solution in toluene. Inset shows a high-magnification image of the boxed area. Reproduced with permission from ref. 145. **b**, Laser confocal fluorescent microscope image of PMMA-PS film obtained by evaporating the solvent from a thin film of the solution of PMMA and PS in toluene. Fluorescent PMMA-rich domains are prominent on the dark background of PS. Scale bar 10  $\mu\text{m}$ . Reproduced with permission from ref. 141. **c**, Schematic representation of electrically induced pattern transfer. Periodicity is induced by the topographically structured electrode. **d**, An AFM image of the topographic pattern produced, as in **(c)**, in brominated PS. Reproduced with permission from ref. 146.

periodicities of patterns obtained from polymer solutions are significantly smaller than those generated under similar conditions in films of simple liquids. Furthermore, the variation in viscosity across films of evaporating polymer solutions can lead to the new phenomenology in pattern formation.

In another instability-driven approach to polymer patterning, application of a high ( $>10^7 \text{ V m}^{-1}$ ) electric field across polymer films at temperatures above the glass-transition temperature of the polymer generated variations in charge density, destabilized the film,

and created lateral and topographic features on it<sup>146</sup>. Instability was governed by the competition between the surface-tension forces acting at the polymer-air interface and forces that arose in response to the polarization of the dielectric polymer layer. For non-patterned electrodes the lateral wavelength,  $\lambda_m$ , of the generated pattern was determined by surface tension,  $\gamma$ , the strength of electric field,  $p_{el}$ , and the thickness of films,  $h$ , as  $\lambda_m = 2\pi[2\gamma/(\partial p_{el}/\partial h)]$ . By using a topographically patterned electrode shown in Fig. 8c, the periodicity of lateral features of the pattern was reduced from 10  $\mu\text{m}$  to 140 nm.

The emerging structure in the film was driven towards protrusions in the electrode yielding a topographic pattern that was a replica of the electrode structure (Fig. 8d).

## CHALLENGES AND THE FUTURE

It is an exciting time for the field of functional polymeric materials. Polymers continue to become increasingly sophisticated, leading to their surface patterns having enhanced specificity or multifunctional tasks. An interdisciplinary approach undertaken by synthetic chemists, polymer and materials scientists, engineers, physicist and biologists helps to develop new polymers that can be patterned with high fidelity and enhanced resolution, without compromising polymer properties. Combinatorial methods are extremely important in this field in planning new and optimizing existing formulations, and in using microarrays of polymers for research and discovery. The use of solvent-free or waterborne polymer formulations is a serious consideration in planning and synthesizing new polymers for surface patterning. Patterning of hybrid polymer-inorganic structures and multilayer structures without cross-talk between the layers remains a challenge.

Some of the applications of polymer-patterned surfaces are still in an early stage, and researchers working in these fields need to acquire knowledge and tools for constructing structures with best performance. For example, it is still not clear how the geometry and porosity of scaffolds affect cell adhesion, growth and behaviour, and how the physical and chemical properties of scaffold polymer materials affect tissue growth.

Patterning surfaces with polymers will move towards the fabrication of more complicated chemical and topological patterns. For example, 3D patterning of polymers for cell deposition has to provide an environment that mimics natural *in vivo* conditions. Spatial localization of different cells and growth factors would allow control of the behaviour of cells. Currently, the fabrication of complex 3D structures with spatial distribution of chemical functionalities remains a challenge.

In the applications of surfaces patterned with polymers associated with microelectronics and optics, two major concerns are to improve patterning efficiency and cost effectiveness, without compromising pattern performance. The challenge is to achieve a balance between high speed and high resolution, and a low-cost patterning process. For example, ink-jet printing has great advantages in the straightforward low-cost patterning of polymers, however, enhanced patterning resolution of this method is compromised by the increased cost of printing. Currently, photolithography is the major technique that is used for high-resolution large-area patterning of polymers; however, this requires clean rooms and expensive equipment, especially when sub-100-nm patterning resolution is desired. Nanoimprinting techniques and BCP lithography are becoming promising alternative strategies in high-resolution patterning of polymers.

In the future, to achieve cost-effective patterning and/or to pattern on multiple length scales, a combination of different patterning techniques will be necessary. For example, the use of both photolithography and printing methods together would allow the fabrication of low-cost organic electronics with enhanced performance. Alternatively, self-assembly of BCPs combined with photolithography would be a route to patterns with different characteristic length scales.

doi:10.1038/nmat2109

## References

- Shimoda, T., Morii, K., Seki, S. & Kiguchi, H. Inkjet printing of light-emitting polymer displays. *Mater. Res. Soc. Bull.* **28**, 821–827 (2003).
- Black, C. T. *et al.* Polymer self assembly in semiconductor microelectronics. *IBM J. Res. Dev.* **51**, 605–633 (2007).
- Singh, T. B. & Sariciftci, N. S. Progress in plastic electronics devices. *Annu. Rev. Mater. Res.* **36**, 199–230 (2006).
- Thery, M. *et al.* The extracellular matrix guides the orientation of the cell division axis. *Nature Cell Biol.* **7**, 947–953 (2005).
- Thery, M. *et al.* Anisotropy of cell adhesive microenvironment governs cell internal organization and orientation of polarity. *Proc. Natl Acad. Sci. USA* **103**, 19771–19776 (2006).
- Hollister, S. J. Porous scaffold design for tissue engineering. *Nature Mater.* **4**, 518–524 (2005).
- Park, M., Harrison, C., Chaikin, P. M., Register, R. A. & Adamson, D. H. Block copolymer lithography: Periodic arrays of  $\sim 10^{11}$  holes in 1 square centimeter. *Science* **276**, 1401–1404 (1997).
- Kane, R. S., Cohen, R. E. & Silbey, R. Synthesis of PbS nanoclusters within block copolymer nanoreactors. *Chem. Mater.* **8**, 1919–1924 (1996).
- Valkama, S. *et al.* Self-assembled polymeric solid films with temperature-induced large and reversible photonic-bandgap switching. *Nature Mater.* **3**, 872–876 (2004).
- Campbell, M., Sharp, D. N., Harrison, M. T., Denning, R. G. & Turberfield, A. J. Fabrication of photonic crystals for the visible spectrum by holographic lithography. *Nature* **404**, 53–56 (2000).
- Fodor, S. P. A. *et al.* Light-directed, spatially addressable parallel chemical synthesis. *Science* **251**, 767–773 (1991).
- Seemann, R., Brinkmann, M., Kramer, E. J., Lange, F. F. & Lipowsky, R. Wetting morphologies at microstructured surfaces. *Proc. Natl Acad. Sci. USA* **102**, 1848–1852 (2005).
- Hammond, P. T. Form and function in multilayer assembly: New applications at the nanoscale. *Adv. Mater.* **16**, 1271–1293 (2004).
- Li, L. J. & Fourkas, J. T. Multiphoton polymerization. *Mater. Today* **10**, 30–37 (2007).
- Moon, J. H., Ford, J. & Yang, S. Fabricating three-dimensional polymeric photonic structures by multi-beam interference lithography. *Polym. Adv. Technol.* **17**, 83–93 (2006).
- Menard, E. *et al.* Micro- and nanopatterning techniques for organic electronic and optoelectronic systems. *Chem. Rev.* **107**, 1117–1160 (2007).
- Kelley, T. W. *et al.* Recent progress in organic electronics: Materials, devices, and processes. *Chem. Mater.* **16**, 4413–4422 (2004).
- Shoji, S. & Kawata, S. Photofabrication of three-dimensional photonic crystals by multibeam laser interference into a photopolymerizable resin. *Appl. Phys. Lett.* **76**, 2668–2670 (2000).
- Bloomstein, T. M. *et al.* Critical issues in 157 nm lithography. *J. Vac. Sci. Technol. B* **16**, 3154–3157 (1998).
- Bloomstein, T. M., Marchant, M. F., Deneault, S., Hardy, D. E. & Rothschild, M. 22-nm immersion interference lithography. *Opt. Express* **14**, 6434–6443 (2006).
- Muller, C. D. *et al.* Multi-colour organic light-emitting displays by solution processing. *Nature* **421**, 829–833 (2003).
- Penterman, R., Klink, S. L., de Koning, H., Nisato, G. & Broer, D. J. Single-substrate liquid-crystal displays by photo-enforced stratification. *Nature* **417**, 55–58 (2002).
- Wu, H. K., Odom, T. W. & Whitesides, G. M. Reduction photolithography using microlens arrays: Applications in gray scale photolithography. *Anal. Chem.* **74**, 3267–3273 (2002).
- Revzin, A., Tompkins, R. G. & Toner, M. Surface engineering with poly(ethylene glycol) photolithography to create high-density cell arrays on glass. *Langmuir* **19**, 9855–9862 (2003).
- Koh, W. G., Revzin, A. & Pishko, M. V. Poly(ethylene glycol) hydrogel microstructures encapsulating living cells. *Langmuir* **18**, 2459–2462 (2002).
- Hoffmann, J., Plotner, M., Kuckling, D. & Fischer, W. J. Photopatterning of thermally sensitive hydrogels useful for microactuators. *Sens. Actuat. A* **77**, 139–144 (1999).
- Lee, M. B. *et al.* Silicon planar-apertured probe array for high-density near-field optical storage. *Appl. Opt.* **38**, 3566–3571 (1999).
- Aldred, M. P. *et al.* A full-color electroluminescent device and patterned photoalignment using light-emitting liquid crystals. *Adv. Mater.* **17**, 1368–1372 (2005).
- Yamato, M., Konno, C., Utsumi, M., Kikuchi, A. & Okano, T. Thermally responsive polymer-grafted surfaces facilitate patterned cell seeding and co-culture. *Biomaterials* **23**, 561–567 (2002).
- Karp, J. M. *et al.* A photolithographic method to create cellular micropatterns. *Biomaterials* **27**, 4755–4764 (2006).
- Hahn, M. S. *et al.* Photolithographic patterning of polyethylene glycol hydrogels. *Biomaterials* **27**, 2519–2524 (2006).
- Albrecht, D. R., Tsang, V. L., Sah, R. L. & Bhatia, S. N. Photo- and electropatterning of hydrogel-encapsulated living cell arrays. *Lab Chip* **5**, 111–118 (2005).
- Albrecht, D. R., Underhill, G. H., Wassermann, T. B., Sah, R. L. & Bhatia, S. N. Probing the role of multicellular organization in three-dimensional microenvironments. *Nature Methods* **3**, 369–375 (2006).
- Kato, K., Tanaka, K., Tsuru, S. & Sakai, S. Reflective color display using polymer-dispersed cholesteric liquid-crystal. *Jpn. J. Appl. Phys.* **33**, 2635–2640 (1994).
- Tondiglia, V. P., Natarajan, L. V., Sutherland, R. L., Tomlin, D. & Bunning, T. J. Holographic formation of electro-optical polymer-liquid crystal photonic crystals. *Adv. Mater.* **14**, 187–191 (2002).
- Miklyayev, Y. V. *et al.* Three-dimensional face-centered-cubic photonic crystal templates by laser lithography: fabrication, optical characterization, and band-structure calculations. *Appl. Phys. Lett.* **82**, 1284–1286 (2003).
- Naydenova, I., Mihaylova, E., Martin, S. & Toal, V. Holographic patterning of acrylamide-based photopolymer surface. *Opt. Express* **13**, 4878–4889 (2005).
- Lai, N. D., Liang, W. P., Lin, J. H., Hsu, C. C. & Lin, C. H. Fabrication of two- and three-dimensional periodic structures by multi-exposure of two-beam interference technique. *Opt. Express* **13**, 9605–9611 (2005).
- Gordon, T. J., Yu, J. F., Yang, C. & Holdcroft, S. Direct thermal patterning of a  $\pi$ -conjugated polymer. *Chem. Mater.* **19**, 2155–2161 (2007).
- Chou, S. Y., Krauss, P. R., Zhang, W., Guo, L. J. & Zhuang, L. Sub-10 nm imprint lithography and applications. *J. Vac. Sci. Technol. B* **15**, 2897–2904 (1997).
- Hua, F. *et al.* Polymer imprint lithography with molecular-scale resolution. *Nano Lett.* **4**, 2467–2471 (2004).
- Guo, L. J. Nanoimprint lithography: Methods and material requirements. *Adv. Mater.* **19**, 495–513 (2007).
- Stewart, M. D. & Willson, C. G. Imprint materials for nanoscale devices. *Mater. Res. Soc. Bull.* **30**, 947–951 (2005).
- Pfeiffer, K. *et al.* Multistep profiles by mix and match of nanoimprint and UV lithography. *Microelectron. Eng.* **57–8**, 381–387 (2001).

45. Behl, M. *et al.* Towards plastic electronics: Patterning semiconducting polymers by nanoimprint lithography. *Adv. Mater.* **14**, 588–591 (2002).
46. Finder, C. *et al.* Fluorescence microscopy for quality control in nanoimprint lithography. *Microelectron. Eng.* **67–8**, 623–628 (2003).
47. Li, H. W. & Huck, W. T. S. Ordered block-copolymer assembly using nanoimprint lithography. *Nano Lett.* **4**, 1633–1636 (2004).
48. Schulz, H. *et al.* New polymer materials for nanoimprinting. *J. Vac. Sci. Technol. B* **18**, 1861–1865 (2000).
49. Nakamatsu, K., Watanabe, K., Tone, K., Namatsu, H. & Matsui, S. Nanoimprint and nanocontact technologies using hydrogen silsesquioxane. *J. Vac. Sci. Technol. B* **23**, 507–512 (2005).
50. Colburn, M. *et al.* Characterization and modeling of volumetric and mechanical properties for step and flash imprint lithography photopolymers. *J. Vac. Sci. Technol. B* **19**, 2685–2689 (2001).
51. Hagberg, E. C., Malkoch, M., Ling, Y. B., Hawker, C. J. & Carter, K. R. Effects of modulus and surface chemistry of thiol-ene photopolymers in nanoimprinting. *Nano Lett.* **7**, 233–237 (2007).
52. Rolland, J. P., Van Dam, R. M., Schorzman, D. A., Quake, S. R. & DeSimone, J. M. Solvent-resistant photocurable “liquid teflon” for microfluidic device fabrication. *J. Am. Chem. Soc.* **126**, 2322–2323 (2004).
53. Schmid, G. M. *et al.* Implementation of an imprint damascene process for interconnect fabrication. *J. Vac. Sci. Technol. B* **24**, 1283–1291 (2006).
54. Mata, A., Fleischnan, A. J. & Roy, S. Fabrication of multi-layer SU-8 microstructures. *J. Micromech. Microeng.* **16**, 276–284 (2006).
55. Kumar, A. & Whitesides, G. M. Features of gold having micrometer to centimeter dimensions can be formed through a combination of stamping with an elastomeric stamp and an alkanethiol ink followed by chemical etching. *Appl. Phys. Lett.* **63**, 2002–2004 (1993).
56. Li, H. W., Muir, B. V. O., Fichet, G. & Huck, W. T. S. Nanocontact printing: A route to sub-50-nm-scale chemical and biological patterning. *Langmuir* **19**, 1963–1965 (2003).
57. Hui, C. Y., Jagota, A., Lin, Y. Y. & Kramer, E. J. Constraints on microcontact printing imposed by stamp deformation. *Langmuir* **18**, 1394–1407 (2002).
58. Sharpe, R. B. A. *et al.* Ink dependence of poly(dimethylsiloxane) contamination in microcontact printing. *Langmuir* **22**, 5945–5951 (2006).
59. Workman, R. K. & Manne, S. Molecular transfer and transport in noncovalent microcontact printing. *Langmuir* **20**, 805–815 (2004).
60. Quist, A. P., Pavlovic, E. & Oscarsson, S. Recent advances in microcontact printing. *Anal. Bioanal. Chem.* **381**, 591–600 (2005).
61. Gates, B. D. *et al.* New approaches to nanofabrication: Molding, printing, and other techniques. *Chem. Rev.* **105**, 1171–1196 (2005).
62. Shah, R. R. *et al.* Using atom transfer radical polymerization to amplify monolayers of initiators patterned by microcontact printing into polymer brushes for pattern transfer. *Macromolecules* **33**, 597–605 (2000).
63. Zhou, F. *et al.* Fabrication of positively patterned conducting polymer microstructures via one-step electrodeposition. *Adv. Mater.* **15**, 1367–1370 (2003).
64. Jiang, X. P., Clark, S. L. & Hammond, P. T. Side-by-side directed multilayer patterning using surface templates. *Adv. Mater.* **13**, 1669–1673 (2001).
65. Park, J., Kim, Y. S. & Hammond, P. T. Chemically nanopatterned surfaces using polyelectrolytes and ultraviolet-cured hard molds. *Nano Lett.* **5**, 1347–1350 (2005).
66. Yan, L., Huck, W. T. S., Zhao, X. M. & Whitesides, G. M. Patterning thin films of poly(ethylene imine) on a reactive SAM using microcontact printing. *Langmuir* **15**, 1208–1214 (1999).
67. Zhou, F., Zheng, Z. J., Yu, B., Liu, W. M. & Huck, W. T. S. Multicomponent polymer brushes. *J. Am. Chem. Soc.* **128**, 16253–16258 (2006).
68. Li, D. W. & Guo, L. J. Micron-scale organic thin film transistors with conducting polymer electrodes patterned by polymer inking and stamping. *Appl. Phys. Lett.* **88** (2006).
69. Kumar, G., Wang, Y. C., Co, C. & Ho, C. C. Spatially controlled cell engineering on biomaterials using polyelectrolytes. *Langmuir* **19**, 10550–10556 (2003).
70. Lin, C. C., Co, C. C. & Ho, C. C. Micropatterning proteins and cells on polylactic acid and poly(lactide-co-glycolide). *Biomaterials* **26**, 3655–3662 (2005).
71. Nyffenegger, R. M. & Penner, R. M. Nanometer-scale surface modification using the scanning probe microscope: Progress since 1991. *Chem. Rev.* **97**, 1195–1230 (1997).
72. Piner, R. D., Zhu, J., Xu, F., Hong, S. H. & Mirkin, C. A. “Dip-pen” nanolithography. *Science* **283**, 661–663 (1999).
73. Hong, S. H., Zhu, J. & Mirkin, C. A. Multiple ink nanolithography: Toward a multiple-pen nano-plotter. *Science* **286**, 523–525 (1999).
74. Hong, S. H. & Mirkin, C. A. A nanoplotter with both parallel and serial writing capabilities. *Science* **288**, 1808–1811 (2000).
75. Lee, K. B., Park, S. J., Mirkin, C. A., Smith, J. C. & Mrksich, M. Protein nanoarrays generated by dip-pen nanolithography. *Science* **295**, 1702–1705 (2002).
76. Xu, P., Uyama, H., Whitten, J. E., Kobayashi, S. & Kaplan, D. L. Peroxidase-catalyzed in situ polymerization of surface oriented caffeic acid. *J. Am. Chem. Soc.* **127**, 11745–11753 (2005).
77. Yang, M., Sheehan, P. E., King, W. P. & Whitman, L. J. Direct writing of a conducting polymer with molecular-level control of physical dimensions and orientation. *J. Am. Chem. Soc.* **128**, 6774–6775 (2006).
78. Lim, J. H. & Mirkin, C. A. Electrostatically driven dip-pen nanolithography of conducting polymers. *Adv. Mater.* **14**, 1474–1477 (2002).
79. McKendry, R. *et al.* Creating nanoscale patterns of dendrimers on silicon surfaces with dip-pen nanolithography. *Nano Lett.* **2**, 713–716 (2002).
80. Salazar, R. B., Shovskiy, A., Schonherr, H. & Vancso, G. J. Dip-pen nanolithography on (bio)reactive monolayer and block-copolymer platforms: Deposition of lines of single macromolecules. *Small* **2**, 1274–1282 (2006).
81. Mamin, H. J. & Rugar, D. Thermomechanical writing with an atomic force microscope tip. *Appl. Phys. Lett.* **61**, 1003–1005 (1992).
82. Maynor, B. W., Filocamo, S. E., Grinstaff, M. W. & Liu, J. Direct-writing of polymer nanostructures: Poly(thiophene) nanowires on semiconducting and insulating surfaces. *J. Am. Chem. Soc.* **124**, 522–523 (2002).
83. Salaita, K. *et al.* Massively parallel dip-pen nanolithography with 55000-pen two-dimensional arrays. *Angew. Chem. Int. Ed.* **45**, 7220–7223 (2006).
84. Vettiger, P. *et al.* The “millipede” - Nanotechnology entering data storage. *IEEE T. Nanotechnol.* **1**, 39–55 (2002).
85. Lee, S. W. *et al.* Biologically active protein nanoarrays generated using parallel dip-pen nanolithography. *Adv. Mater.* **18**, 1133–1136 (2006).
86. Siringhaus, H. *et al.* High-resolution inkjet printing of all-polymer transistor circuits. *Science* **290**, 2123–2126 (2000).
87. Bonaccorso, E., Butt, H. J., Hankeln, B., Niesenhaus, B. & Graf, K. Fabrication of microvessels and microlenses from polymers by solvent droplets. *Appl. Phys. Lett.* **86** (2005).
88. Sele, C. W., von Werne, T., Friend, R. H. & Siringhaus, H. Lithography-free, self-aligned inkjet printing with sub-hundred-nanometer resolution. *Adv. Mater.* **17**, 997–1001 (2005).
89. Park, J. U. *et al.* High-resolution electrohydrodynamic jet printing. *Nature Mater.* **6**, 782–789 (2007).
90. Christanti, Y. & Walker, L. M. Surface tension driven jet break up of strain-hardening polymer solutions. *J. Non-Newtonian Fluid Mech.* **100**, 9–26 (2001).
91. Carter, J. C. *et al.* Fabricating optical fiber imaging sensors using inkjet printing technology: A pH sensor proof-of-concept. *Biosens. Bioelectron.* **21**, 1359–1364 (2006).
92. Roth, E. A. *et al.* Inkjet printing for high-throughput cell patterning. *Biomaterials* **25**, 3707–3715 (2004).
93. Vozzi, G., Previti, A., De Rossi, D. & Ahluwalia, A. Microsyringe-based deposition of two-dimensional and three-dimensional polymer scaffolds with a well-defined geometry for application to tissue engineering. *Tissue Eng.* **8**, 1089–1098 (2002).
94. Vozzi, G., Flaim, C., Ahluwalia, A. & Bhatia, S. Fabrication of PLGA scaffolds using soft lithography and microsyringe deposition. *Biomaterials* **24**, 2533–2540 (2003).
95. Woodfield, T. B. F. *et al.* Design of porous scaffolds for cartilage tissue engineering using a three-dimensional fiber-deposition technique. *Biomaterials* **25**, 4149–4161 (2004).
96. Landers, R., Hubner, U., Schmelzeisen, R. & Mulhaupt, R. Rapid prototyping of scaffolds derived from thermoreversible hydrogels and tailored for applications in tissue engineering. *Biomaterials* **23**, 4437–4447 (2002).
97. Geng, L. *et al.* Direct writing of chitosan scaffolds using a robotic system. *Rapid Prototyping J.* **11**, 90–97 (2005).
98. Gratson, G. M., Xu, M. J. & Lewis, J. A. Microperiodic structures: Direct writing of three-dimensional webs. *Nature* **428**, 386–386 (2004).
99. Theriault, D., White, S. R. & Lewis, J. A. Chaotic mixing in three-dimensional microvascular networks fabricated by direct-write assembly. *Nature Mater.* **2**, 265–271 (2003).
100. Xu, M. J., Gratson, G. M., Duoss, E. B., Shepherd, R. F. & Lewis, J. A. Biomimetic silicification of 3D polyamine-rich scaffolds assembled by direct ink writing. *Soft Matter* **2**, 205–209 (2006).
101. Gratson, G. M. *et al.* Direct-write assembly of three-dimensional photonic crystals: Conversion of polymer scaffolds to silicon hollow-woodpile structures. *Adv. Mater.* **18**, 461–465 (2006).
102. Hutmacher, D. W. Scaffolds in tissue engineering bone and cartilage. *Biomaterials* **21**, 2529–2543 (2000).
103. Endres, M. *et al.* Osteogenic induction of human bone marrow-derived mesenchymal progenitor cells in novel synthetic polymer-hydrogel matrices. *Tissue Eng.* **9**, 689–702 (2003).
104. Li, M. Q., Coenjarts, C. A. & Ober, C. K. In *Block Copolymers II* (ed. Abetz, V.) 183–226 (Advances in Polymer Science Series Vol. 190, Springer, Berlin, 2005).
105. Kim, G. & Libera, M. Morphological development in solvent-cast polystyrene-polybutadiene-polystyrene (SBS) triblock copolymer thin films. *Macromolecules* **31**, 2569–2577 (1998).
106. Bang, J. *et al.* Effect of humidity on the ordering of PEO-based copolymer thin films. *Macromolecules* **40**, 7019–7025 (2007).
107. Fasolka, M. J. & Mayes, A. M. Block copolymer thin films: Physics and applications. *Annu. Rev. Mater. Res.* **31**, 323–355 (2001).
108. Kim, S. H., Misner, M. J., Xu, T., Kimura, M. & Russell, T. P. Highly oriented and ordered arrays from block copolymers via solvent evaporation. *Adv. Mater.* **16**, 226–231 (2004).
109. Segalman, R. A., Yokoyama, H. & Kramer, E. J. Graphoepitaxy of spherical domain block copolymer films. *Adv. Mater.* **13**, 1152–1155 (2001).
110. Cheng, J. Y., Mayes, A. M. & Ross, C. A. Nanostructure engineering by templated self-assembly of block copolymers. *Nature Mater.* **3**, 823–828 (2004).
111. Kim, S. O. *et al.* Epitaxial self-assembly of block copolymers on lithographically defined nanopatterned substrates. *Nature* **424**, 411–414 (2003).
112. Stoykovich, M. P. *et al.* Directed assembly of block copolymer blends into nonregular device-oriented structures. *Science* **308**, 1442–1446 (2005).
113. Angelescu, D. E. *et al.* Macroscopic orientation of block copolymer cylinders in single-layer films by shearing. *Adv. Mater.* **16**, 1736–1740 (2004).
114. Osuji, C. *et al.* Alignment of self-assembled hierarchical microstructure in liquid crystalline diblock copolymers using high magnetic fields. *Macromolecules* **37**, 9903–9908 (2004).
115. Xu, T., Zhu, Y. Q., Gido, S. P. & Russell, T. P. Electric field alignment of symmetric diblock copolymer thin films. *Macromolecules* **37**, 2625–2629 (2004).
116. Harrison, C. *et al.* Dynamics of pattern coarsening in a two-dimensional smectic system. *Phys. Rev. E* **66**, 011706 (2002).
117. Fukunaga, K., Elbs, H., Magerle, R. & Krausch, G. Large-scale alignment of ABC block copolymer microdomains via solvent vapor treatment. *Macromolecules* **33**, 947–953 (2000).
118. Du, P. *et al.* Additive-driven phase-selective chemistry in block copolymer thin films: The convergence of top-down and bottom-up approaches. *Adv. Mater.* **16**, 953–957 (2004).
119. Kim, D. H. *et al.* Thin films of block copolymers as planar optical waveguides. *Adv. Mater.* **17**, 2442–2446 (2005).
120. Xu, C., Wayland, B. B., Fryd, M., Winey, K. I. & Composto, R. J. pH-responsive nanostructures assembled from amphiphilic block copolymers. *Macromolecules* **39**, 6063–6070 (2006).
121. Yang, S. Y. *et al.* Nanoporous membranes with ultrahigh selectivity and flux for the filtration of viruses. *Adv. Mater.* **18**, 709–712 (2006).
122. Shin, K. *et al.* A simple route to metal nanodots and nanoporous metal films. *Nano Lett.* **2**, 933–936 (2002).
123. Urbas, A. *et al.* Tunable block copolymer/homopolymer photonic crystals. *Adv. Mater.* **12**, 812–814 (2000).

124. Bockstaller, M., Kolb, R. & Thomas, E. L. Metallo-dielectric photonic crystals based on diblock copolymers. *Adv. Mater.* **13**, 1783–1786 (2001).
125. Urbas, A. M., Maldovan, M., DeRege, P. & Thomas, E. L. Bicontinuous cubic block copolymer photonic crystals. *Adv. Mater.* **14**, 1850–1853 (2002).
126. Chan, V. Z. H. *et al.* Ordered bicontinuous nanoporous and nanorelief ceramic films from self-assembling polymer precursors. *Science* **286**, 1716–1719 (1999).
127. Cheng, J. Y. *et al.* Formation of a cobalt magnetic dot array via block copolymer lithography. *Adv. Mater.* **13**, 1174–1178 (2001).
128. Kim, H. C. *et al.* A route to nanoscopic SiO<sub>2</sub> posts via block copolymer templates. *Adv. Mater.* **13**, 795–797 (2001).
129. Xu, T. *et al.* Block copolymer surface reconstruction: A reversible route to nanoporous films. *Adv. Funct. Mater.* **13**, 698–702 (2003).
130. Hashimoto, T., Tsutsumi, K. & Funaki, Y. Nanoprocessing based on bicontinuous microdomains of block copolymers: Nanochannels coated with metals. *Langmuir* **13**, 6869–6872 (1997).
131. Black, C. T. *et al.* Integration of self-assembled diblock copolymers for semiconductor capacitor fabrication. *Appl. Phys. Lett.* **79**, 409–411 (2001).
132. Black, C. T. *et al.* High-capacity, self-assembled metal-oxide-semiconductor decoupling capacitors. *IEEE Electron Device Lett.* **25**, 622–624 (2004).
133. Zschech, D. *et al.* Ordered arrays of <100>-oriented silicon nanorods by CMOS-compatible block copolymer lithography. *Nano Lett.* **7**, 1516–1520 (2007).
134. Thurn-Albrecht, T. *et al.* Ultrahigh-density nanowire arrays grown in self-assembled diblock copolymer templates. *Science* **290**, 2126–2129 (2000).
135. Kim, D. H., Lin, Z. Q., Kim, H. C., Jeong, U. & Russell, T. P. On the replication of block copolymer templates by poly(dimethylsiloxane) elastomers. *Adv. Mater.* **15**, 811–814 (2003).
136. Temple, K. *et al.* Spontaneous vertical ordering and pyrolytic formation of nanoscopic ceramic patterns from poly(styrene-*b*-ferrocenylsilane). *Adv. Mater.* **15**, 297–300 (2003).
137. Kim, D. H., Kim, S. H., Lavery, K. & Russell, T. P. Inorganic nanodots from thin films of block copolymers. *Nano Lett.* **4**, 1841–1844 (2004).
138. Lin, Y. *et al.* Self-directed self-assembly of nanoparticle/copolymer mixtures. *Nature* **434**, 55–59 (2005).
139. Lopes, W. A. & Jaeger, H. M. Hierarchical self-assembly of metal nanostructures on diblock copolymer scaffolds. *Nature* **414**, 735–738 (2001).
140. Bodenschatz, E., Pesch, W. & Ahlers, G. Recent developments in Rayleigh-Benard convection. *Annu. Rev. Fluid Mech.* **32**, 709–778 (2000).
141. Mitov, Z. & Kumacheva, E. Convection-induced patterns in phase-separating polymeric fluids. *Phys. Rev. Lett.* **81**, 3427–3430 (1998).
142. Xu, S. Q. & Kumacheva, E. Ordered morphologies in polymeric films produced by replication of convection patterns. *J. Am. Chem. Soc.* **124**, 1142–1143 (2002).
143. Li, M. Q., Xu, S. Q. & Kumacheva, E. Convection patterns trapped in the solid state by UV-induced polymerization. *Langmuir* **16**, 7275–7278 (2000).
144. Li, M. Q., Xu, S. Q. & Kumacheva, E. Convection in polymeric fluids subjected to vertical temperature gradients. *Macromolecules* **33**, 4972–4978 (2000).
145. Srinivasarao, M., Collings, D., Philips, A. & Patel, S. Three-dimensionally ordered array of air bubbles in a polymer film. *Science* **292**, 79–83 (2001).
146. Schaffer, E., Thurn-Albrecht, T., Russell, T. P. & Steiner, U. Electrically induced structure formation and pattern transfer. *Nature* **403**, 874–877 (2000).